Magnesium Technology 2011
Edited by: Wim H. Sillekens, Sean R. Agnew, Neale R. Neelameggham, and Suveen N. Mathaudhu
TMS (The Minerals, Metals & Materials Society), 2011

THE EFFECT OF THERMOMECHANICAL PROCESSING ON THE CREEP BEHAVIOR AND FRACTURE TOUGHNESS OF THIXOMOLDED® AM60 ALLOY

Z. Chen[1], J. Huang[2], R. Decker[2], S. LeBeau[2], and C.J. Boehlert[1]

[1]Michigan State University, East Lansing, Michigan, 48824
[2]Thixomat, Incorporated, Ann Arbor, Michigan, 48108

Keywords: Magnesium, Lightweight Alloys, Creep, Fracture Toughness

Abstract

Creep and fracture toughness experiments were performed on a commercially available magnesium-aluminum alloy (AM60) after three processing treatments: (1) As-Thixomolded® (as-molded), (2) Thixomolded® then thermomechanically processed (TTMP), and (3) Thixomolded® then TTMP then annealed (annealed). The conventional tensile-creep experiments were performed at applied stresses ranging between 20-75MPa and temperatures between 373-473K (100-200°C). *In-situ* tensile-creep tests were performed on selected samples. The as-molded material exhibited creep resistance superior to the thermomechanically processed materials. Creep experiments indicated grain boundary cracking, and grain size was expected to be an important microstructural parameter that affected the creep behavior. Fracture toughness experiments were performed at room temperature (RT) on single edge notched tension (SENT) samples. The TTMP and annealed materials exhibited fracture toughness values almost twice that of the as-molded material.

Introduction

With increasing fuel cost and global environmental awareness, the demand for lightweight structural materials to increase fuel efficiency is paramount in the automotive industry. Magnesium (Mg) alloys have low density and exhibit high specific strengths. Thus, they serve as attractive candidate for replacing the Al alloys widely used in automotive industry. Previous work by our group was conducted to investigate the RT and elevated-temperature tensile and fatigue properties of a Thixomolded® AM60 alloy processed under different conditions [1]. This study focused on the effect of thermomechanical processing on the creep behavior and fracture toughness of the Thixomolded® AM60 alloy.

Experimental

The measured bulk chemical composition of the as-molded material is shown in Table I. The AM60 alloy was thixomolded into 3.2mm thick plates which represented the as-molded condition [2]. Some of the plates were then thermomechanically processed in order to induce dynamic recrystallization and this represented the TTMP condition. Several of the thermomechanically-processed plates were then annealed and this represented the annealed condition.

Conventional tensile-creep tests were performed using vertical load frames manufactured by Applied Test System, Incorporated (Butler, PA). Flat dogbone-shaped samples, containing a gage length of 25mm and a gage width of 12mm, were electro-discharge machined, and polished using 600 grit silicon carbide paper to remove the recast layers before testing. Test temperatures were ranged between 373-473K (100-200°C), and targeted test temperatures were maintained within ±3K. Applied stresses ranged between 20-75MPa. Strain was measured and documented throughout the test, by a linear variable differential transformer on a high temperature extensometer. After a minimum strain rate was achieved, either the load or temperature was increased or the test was stopped. Upon termination of the creep experiments, the samples remained under load while the temperature was decreased in order to maintain the deformed state of the sample. Several of the deformed gage sections were cut and polished using silicon carbide paper and diamond paste to a final finish of 0.25μm with ethanol as a lubricant, and then observed using a JEOL 6500 Field Emission scanning electron microscope (SEM).

Table I. Chemical composition in wt% of the studied AM60 alloy.

Al	Mn	Zn	Fe	Si	Ni	Be	Mg
6.29	0.28	0.05	0.001	0.02	0.0009	0.0007	93.34

In-situ tensile-creep experiments were conducted on the annealed material. Flat dogbone-shaped samples, with gage dimensions of 3mm wide by 2.5mm thick by 10mm long, were EDM cut. The specimens were glued to a metallic platen and polished to a 1μm finish using an automatic polishing machine and ethanol as a polishing lubricant. These experiments were performed using a screw-driven tensile stage (built by Ernest F. Fullam, Incorporated, which was purchased by MTI, Inc.) placed inside an Xl-30 FEG FEI SEM. Temperature was controlled using a constant-voltage power supply to a 6mm diameter tungsten-based heater located just below the gage section of the sample. An open-bath, closed-loop chiller was used to circulate distilled water at RT through copper tubes to prevent the tensile stage from overheating. A fine-gage K-type thermocouple was spot-welded to the gage section of each sample. After the sample's gage-section temperature reached the desired creep temperature, a 30 minute period was given to stabilize the thermal stress prior to applying load. The load, which was measured using a 4,448 N load cell, was applied at 3.7N/s until reaching the desired creep stress. The tests were considered constant load where the stress fluctuation varied ±3MPa. The displacement data acquired during the experiments included that of the sample as well as the gripping fixtures. Thus the displacement values reported do not represent the sole displacement of the reduced gage section of the sample. Secondary electron SEM images were taken before loading and at periodic displacements throughout the creep experiments without interrupting the experiment. The pressure in the SEM chamber never exceeded 10^{-6} torr, and therefore oxidation did not detrimentally affect the SEM imaging. Further details of this apparatus and testing technique can be found elsewhere [3-5].

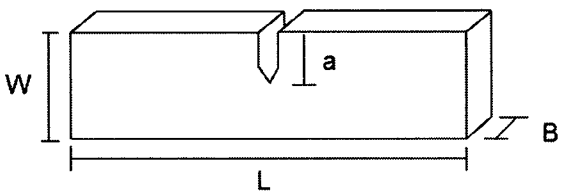

Figure 1. Illustration of SNTT sample.

Fracture toughness experiments were also performed at RT using a servohydraulic system [6]. SENT samples were EDM machined and the geometry of the sample is shown in Figure 1, where width W=12.5mm; crack length a=7mm; thickness B=3.2mm for as-molded material, and B=1.6mm for the TTMP and annealed materials. The longitudinal direction of the specimen was parallel to the longitudinal direction of the plates. The specimen surfaces were polished using silicon carbide paper to reduce the effects of surface defects. No fatigue precrack was introduced and the initial precrack (introduced through EDM) length a was measured using digital imaging. The samples were loaded in tension at a 75N/s loading rate for the TTMP and annealed materials, and at 150N/s for the as-molded material. The crack opening displacement was measured using an extensometer attached to the specimen. Two experiments were performed for each material.

Results

Previous study showed that the as-molded material exhibited an equiaxed α grain morphology where the $Mg_{17}Al_{12}$ β phase decorated the grain boundary [1]. The thermomechanical processing induced a finer grain size and strong basal texture to the TTMP and annealed material. The TTMP material exhibited the highest strength while the annealed material exhibited an intermediate strength but the highest elongation-to-failure (ε_f) More information can be found in reference [1].

Creep

The creep behavior resembled that typical for pure metals indicating three stages of creep. Creep strain versus time curves for the studied AM60 alloys tested under three different applied stress levels at 423K (150°C) are shown in Figure 2. The minimum creep rate versus stress plots for the studied AM60 alloys are shown in Figure 3. The creep stress exponents (n) can be calculated based on these plots, and the n values at 423K (150°C) were 4.9, 5.8, and 4.5 for the as-molded, TTMP, and annealed materials, respectively. Figure 4 shows the temperature dependence of the minimum creep rate under 20MPa applied stress, and the apparent activation energy (Q_{app}) was calculated based on this plot. The plot showed a two-stage linear relationship. Between 373-423K (100-150°C), the Q_{app} for the as-molded, TTMP, and annealed materials were 48kJ/mol, 64kJ/mol and 67kJ/mol, respectively. Between 423-473K (150-200°C), the Q_{app} for the as-molded, TTMP, and annealed materials were 128kJ/mol, 174kJ/mol, and 126kJ/mol, respectively. Grain boundaries served as crack nucleation sites in creep, see Figure 5.

The *in-situ* creep experiments highlighted the surface grain boundary cracking, see Figures 6 and 7. It appeared that the grain

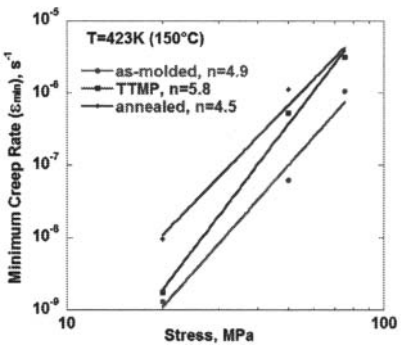

Figure 3. Minimum creep rate versus stress plot at T=423K (150°C) for the studied AM60 alloys. The creep stress exponent (n) values are shown.

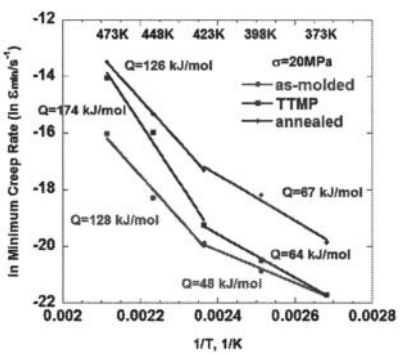

Figure 4. ln minimum creep rate versus reciprocal of temperature plot for the studied AM60 alloys at σ=20MPa. The apparent creep activation energy (Q_{app}) values are shown.

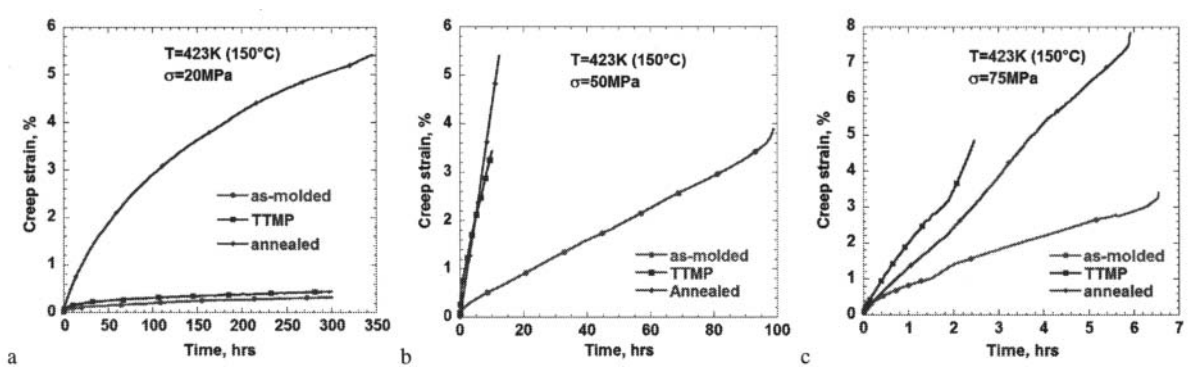

Figure 2. Creep strain versus time plot of the studied materials at 423K (150°C): (a) σ=20MPa, (b) σ=50MPa, and (c) σ=75MPa.

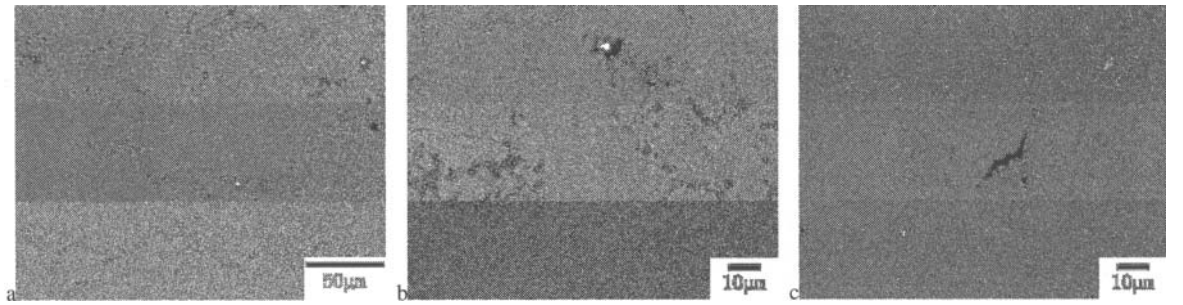

Figure 5. Backscattered electron images of the subsurface for creep tested samples: (a) as-molded sample, tested at 20MPa, 373-473K (100-200°C), total strain was 2.3%, (b) TTMP sample, tested at 75MPa, 423K (150°C), total strain was 4.8%, (c) annealed sample, tested at 20MPa, 373-473K (100-200°C), total strain was 10.5%

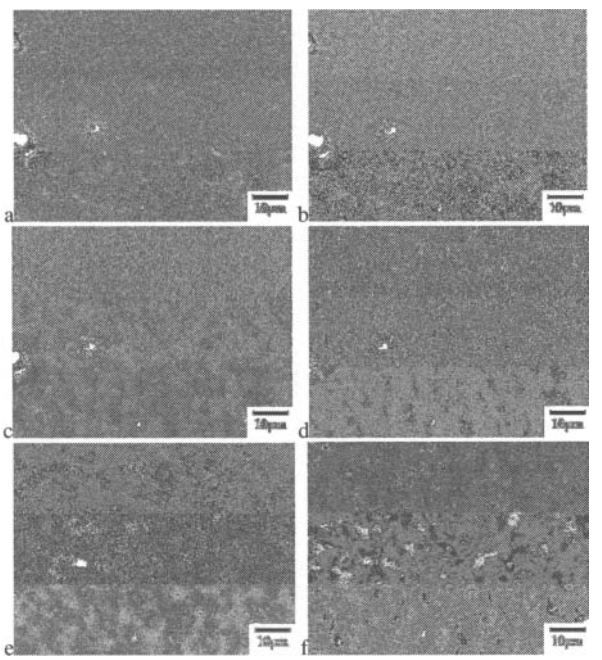

Figure 6. Secondary electron images of an annealed sample taken during an *in-situ* creep test at 50MPa and 423K (150°C). The displacements were (a) 0.168mm, (b) 0.328mm, (c) 0.579mm, (d) 0.945mm, (e) 1.730mm, (f) 2.553mm. A significant amount of grain boundary cracking was evident.

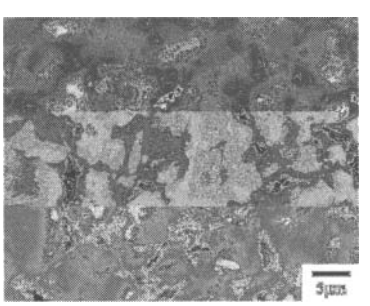

Figure 7. Secondary electron images of the surface of an annealed sample after *in-situ* creep testing at 423K (150°C) and 75MPa. The final displacement was 3.127mm.

boundary cracking was associated with grain boundary sliding as surface fiducial scratches were jogged at grain boundary locations, see Figure 7. Thus grain boundary cracking may have been accommodating the grain boundary sliding.

Fracture Toughness

The fracture toughness was calculated according to the following equations [7]:

$$f(\frac{a}{W}) = \frac{K_Q B\sqrt{W}}{P_Q}, \quad (1)$$

where for the SENT geometry:

$$f(\frac{a}{W}) = \frac{\sqrt{2\tan\frac{\pi a}{2W}}}{\cos\frac{\pi a}{2W}}[0.752 + 2.02(\frac{a}{W}) + 0.37(1-\sin\frac{\pi a}{2W})^3] \quad (2)$$

P_Q is the critical load when fracture occurred and was determined from the load-displacement relationship according to ASTM E 399 [8]. Table II summarizes the fracture toughness data. Although the P_{max}/P_Q ratio exceeded 1.10, the conditional fracture toughness K_Q was calculated based on the P_Q value. The K_Q value was then used to estimate the minimum thickness of the sample necessary for a valid plane-strain fracture toughness test, based on the relationship suggested by ASTM E 399:

$$B, a, W - a > 2.5(\frac{K_Q}{\sigma_{ys}}) \quad (3)$$

As shown in Table II, the actual sample thickness was significantly smaller than that necessary for achieving plane-strain conditions.

Discussion

Creep

The as-molded material exhibited the lowest creep strain rates, see Figures 2-4. The reason for this might be that the TTMP and annealed materials both had smaller grain size than the as-molded material. The TTMP material exhibited a lower minimum creep rate than the annealed material at applied stresses of 20MPa and 50MPa. However this was not the case at an applied stress of 75MPa. The reason for this crossover is not clear and will be the subject of further investigation.

Table II. Summary of the fracture toughness measurements.

Condition	Specimen ID	P_Q,N	Pmax,N	P_{max}/P_Q	f(a/w)	K_Q,MPam$^{0.5}$	B_{min} for valid K_{IC}, mm
As-molded	A	1128	2276	2.01	4.61	15.0	32.6
	B	1322	2295	1.74	4.64	17.5	44.7
TTMP	A	1111	1288	1.16	4.76	31.8	23.1
	B	1012	1328	1.31	4.61	27.9	17.8
Annealed	A	1012	1614	1.59	4.59	27.4	36.4
	B	1021	1596	1.56	4.66	28.1	38.2

The measured creep exponents imply dislocation climb to be the dominant mechanism controlling the secondary creep rate. Similar creep exponents have been reported for QE22 (Mg-2Ag-2Nd) [9], Mg-Y alloys [10], Mg-Zn-Zr alloys [11], and die cast AZ91D and AS21 [12]. In both ingot and die cast AZ91, creep mechanisms based on dislocation motion (on basal and non-basal planes) were proposed [13, 14], where the ingot exhibited a creep rate one order of magnitude lower than the die cast alloy which was proposed to be due to the larger grain size in the ingot microstructure. During creep of Mg-5.6Y-0.04Zn(wt.%) (Mg-1.6mol%Y-0.015mol%Zn), bowed out dislocations were observed to trail straight dislocation segments parallel to the trace of basal planes [10]. The bowed-out dislocations were moving on prismatic planes. The deformation observations in the current work suggest grain boundary sliding also contributed significantly to the strain rates, see Figures 5-7, where grain boundary cracking may have been accommodating the grain boundary sliding. Thus, these two creep deformation processes may be competing and the measured activation energy suggest that temperature may have an influence on this competition.

For temperatures above 423K (150°C), the measured activation energy resembled that for lattice self diffusion [15], while for temperatures less than 423K (150°C), the activation energies were roughly half that for lattice self diffusion. This suggests that grain boundary diffusion may be dominant at lower temperatures. The measured Q_{app} values in low-temperature regime were in good agreement with previous measurements of particle strengthened Mg alloys [11, 12]. Dargusch and Dunlop [12] reported Q_{app} values between 36-44kJ/mol for creep of AZ91D and AS21 and related it to the grain boundary sliding mechanism promoted by discontinuous precipitation of $Mg_{17}Al_{12}$ for which the activation energy is 30kJ/mol [16]. For the high-temperature creep regime (423-473K (150-200°C)), the measured Q_{app} values were close to the 125kJ/mol measured for high-temperature creep of pure Mg, and in the range of 92-135 kJ/mol reported for the activation energy for dislocation glide in basal planes in pure Mg which is also the self-diffusion activation energy in the Mg lattice [15]. In addition, others have measured Q_{app} values between 120-143kJ/mol in the high-temperature regime [17]. The grain boundary cracking and grain boundary sliding observations were made at the transition temperature (423K (150°C)) between the high-temperature and low-temperature regimes. It is expected that the equiaxed α grain size is an important microstructural feature, especially at temperatures of 423K (150°C) and below. The refinement caused by the TMP process would be expected to decrease the creep resistance. Thus grain size appeared to have an influence on the creep behavior. This is a strong consideration for the implementation of TMP Thixomolded® Mg alloys in creep-driven applications, such as automotive engine applications which are subjected to elevated temperatures.

Fracture Toughness

According to Table II, the SENT sample thicknesses were well below those required for valid plane-strain fracture toughness condition. Thus the K_Q values should not be interpreted as plane-strain fracture toughness K_{IC}. The K_Q values for the TTMP and annealed materials were similar, and they were roughly twice that of the as-molded materials. Thus the TMP treatment significantly improved the fracture toughness and this was considered to be related to the significantly higher tensile strength achieved in the TTMP material and the significantly higher ε_f value achieved in the annealed material as compared to the as-molded material [1].

Conclusions

1. The creep resistance of the as-molded material was superior to the thermomechanically processed materials. The creep experiments indicated cracking preferentially occurred at grain boundaries. Grain size was expected to be an important microstructural parameter, and this partially explains why the creep resistance of the as-molded material was superior to that for the thermomechanically processed materials.

2. Through thermomechanical treatment of AM60, the fracture toughness can be almost doubled.

Acknowledgement

This research was conducted in part through the Oak Ridge National Laboratory's High Temperature Materials Laboratory User Program, which is sponsored by the U. S. Department of Energy, Office of Energy Efficiency and Renewable Energy, Vehicle Technologies Program, and through the Oak Ridge National Laboratory's SHaRE User Facility, which is sponsored by the Division of Scientific User Facilities, Office of Basic Energy Sciences, U.S. Department of Energy. A portion of this work was supported by the Faculty and Student Teams (FAST) Program, which is a cooperative program between the Department of Energy Office of Science and the National Science Foundation. The authors are grateful to Mr. Bryan Kuhr and Mr. Alex Ritter of Michigan State University for their technical assistance with the SEM, and *in-situ* deformation characterization

References

1. Chen, Z., et al., *The Effect of Thermomechanical Processing on the Tensile and Fatigue Behavior of Thixomolded(R) AM60*, in *Magnesium Technology 2010*, S.R. Agnew, et al., Editors. 2010, TMS: Seattle. p. 495-500.
2. Decker, R.F., et al., *Magnesium Semi-Solid Metal Forming.* Advanced Materials & Processes, 1996. **149**(2): p. 41-42.
3. Boehlert, C.J., et al., *In situ Scanning Electron Microscopy Observations of Tensile Deformation in a Boron-Modified Ti-6Al-4V Alloy.* Scripta Materialia, 2006. **55**(5): p. 465-468.
4. Cowen, C.J. and C.J. Boehlert, *Comparison of the Microstructure, Tensile, and Creep Behavior for Ti-22Al-26Nb (at. pct) and Ti-22Al-26Nb-5B (at. pct).* Metallurgical and Materials Transactions a-Physical Metallurgy and Materials Science, 2007. **38A**(1): p. 26-34.
5. Quast, J.P. and C.J. Boehlert, *Comparison of the Microstructure, Tensile, and Creep Behavior for Ti-24Al-17Nb-0.66Mo (atomic percent) and Ti-24Al-17Nb-2.3Mo (atomic percent) Alloys.* Metallurgical and Materials Transactions a-Physical Metallurgy and Materials Science, 2007. **38A**(3): p. 529-536.
6. Hartman, G.A. and S.M. Russ, *Techniques for Mechanical and Thermal Testing of Ti3Al/SCS-6 Metal Matrix Composites*, in *Metal Matrix Composites: Testing, Analysis and Failure Modes*, W.S. Johnson, Editor. 1989, American Society for Testing and Materials: Philadelphia, PA. p. 43-53.
7. Anderson, T.L., *Fracture Mechanics: Fundamentals and Applications.* 1991, Boca Raton, FL: CRC Press, Inc. 793.
8. *Standard Test Method for Plane-Strain Fracture Toughness of Metallic Materials*, in *Annual Book of ASTM Standards, vol. 03.01.* 2000, American Society for Testing and Materials: Philadelphia, PA. p. 431-461.
9. Mordike, R.L. and P. Lukac. in *Proceedings of the 3rd International Magnesium Conference.* 1997. London, England: The Institute of Metals.
10. Maruyama, K., M. Suzuki, and H. Sato, *Creep Strength of Magnesium-Based Alloys.* Metallurgical and Materials Transactions a-Physical Metallurgy and Materials Science, 2002. **33**(3): p. 875-882.
11. Boehlert, C.J., *The Tensile and Creep Behavior of Mg-Zn Alloys with and without Y and Zr as Ternary Elements.* Journal of Materials Science, 2007. **42**(10): p. 3675-3684.
12. Dargusch, M.S. and G.L. Dunlop, in *Magnesium Alloys and Their Applications*, B.L. Mordike and K.U. Kainer, Editors. 1998, Werkstoff-Informationsgesellschaft: Frankfurt, Germany. p. 277-282.
13. Regev, M., et al., *Creep Studies of Coarse-Grained AZ91D Magnesium Castings.* Materials Science and Engineering a-Structural Materials Properties Microstructure and Processing, 1998. **252**(1): p. 6-16.
14. Regev, M., E. Aghion, and A. Rosen, *Creep Studies of AZ91D Pressure Die Casting.* Materials Science and Engineering a-Structural Materials Properties Microstructure and Processing, 1997. **234**: p. 123-126.
15. Dieter, G.E., *Mechanical Metallurgy.* 1986, New York: McGraw-Hill.
16. Uchida, H. and T. Shinya, J. Jpn. Inst. Light Metals, 1995. **45**(10): p. 572.
17. Vagarali, S.S. and T.G. Langdon, *Deformation Mechanisms in Hcp Metals at Elevated-Temperatures .2. Creep-Behavior of a Mg-0.8-Percent Al Solid-Solution Alloy.* Acta Metallurgica, 1982. **30**(6): p. 1157-1170.